Investigation of Plasma Parameters at BATMAN for Variation of the Cs Evaporation Asymmetry and Comparing Two Driver Geometries

C. Wimmer[a)], U. Fantz, E. Aza, J. Jovović, W. Kraus, A. Mimo, L. Schiesko and the NNBI-Team

Max-Planck-Institut für Plasmaphysik, Boltzmannstr. 2, 85748 Garching, Germany

[a)]Corresponding author: christian.wimmer@ipp.mpg.de

Abstract. The Neutral Beam Injection (NBI) system for fusion devices like ITER and, beyond ITER, DEMO requires large scale sources for negative hydrogen ions. BATMAN (Bavarian Test Machine for Negative ions) is a test facility attached with the prototype source for the ITER NBI (1/8 source size of the ITER source), dedicated to physical investigations due to its flexible access for diagnostics and exchange of source components. The required amount of negative ions is produced by surface conversion of hydrogen atoms or ions on caesiated surfaces. Several diagnostic tools (Optical Emission Spectroscopy, Cavity Ring-Down Spectroscopy for H^-, Langmuir probes, Tunable Diode Laser Absorption Spectroscopy for Cs) allow the determination of plasma parameters in the ion source. Plasma parameters for two modifications of the standard prototype source have been investigated:

Firstly, a second Cs oven has been installed in the bottom part of the back plate in addition to the regularly used oven in the top part of the back plate. Evaporation from the top oven only can lead to a vertically asymmetric Cs distribution in front of the plasma grid. Using both ovens, a symmetric Cs distribution can be reached – however, in most cases no significant change of the extracted ion current has been determined for varying Cs symmetry if the source is well-conditioned.

Secondly, BATMAN has been equipped with a much larger, racetrack-shaped RF driver (area of 32x58 cm^2) instead of the cylindrical RF driver (diameter of 24.5 cm). The main idea is that one racetrack driver could substitute two cylindrical drivers in larger sources with increased reliability and power efficiency. For the same applied RF power, the electron density is lower in the racetrack driver due to its five times higher volume. The fraction of hydrogen atoms to molecules, however, is at a similar level or even slightly higher, which is a promising result for application in larger sources.

INTRODUCTION

Large and powerful sources for negative hydrogen ions, which are able to deliver a current of 57 A D^- and 66 A H^-, respectively, are required for the neutral beam injection (NBI) system of the upcoming ITER fusion device [1, 2], and beyond ITER, for DEMO. The prototype RF source [3] has become the ITER reference design in 2007 [4]. The production of H^- takes place by the surface process [5] on a Cs-covered (low work function) grid (plasma grid, PG) by conversion of mainly hydrogen atoms [6] to negative ions. Hydrogen atoms are created by dissociation of molecules in a RF heated driver (cylindric shape, diameter of 24.5 cm) in plasma environment (electron temperature of $T_e \approx 10$ eV, electron density $\approx 10^{18}$ m^{-3}). Negative ions are extracted out of the source plasma by a three-grid extraction system; inevitably co-extracted electrons are removed prior full acceleration using magnets installed in the second grid (extraction grid, EG), deflecting electrons directly onto this grid. The created heat load on the EG limits the tolerable amount of co-extracted electrons. In order to minimize the H^- destruction process by electron stripping, it is required to reduce the electron temperature in front of the plasma grid. For this purpose, an expansion chamber with a horizontal magnetic filter field applied (created by permanent magnets) cools down the plasma to an electron temperature of $T_e \approx 1$ eV close to extraction system and in addition lowers the electron density. The horizontal magnetic filter field creates $\vec{F}\times\vec{B}$ drifts in the expansion volume, leading to a vertically asymmetric plasma distribution in front of the PG [7]. Since the Cs coverage of the PG can quickly deteriorate under the vacuum conditions present in the source ($p \approx 1 \times 10^{-6}$ mbar), usually a continuous evaporation of Cs into the source is required during operation. For this purpose, a Cs oven is mounted in the top part of the expansion chamber back plate in the prototype source.

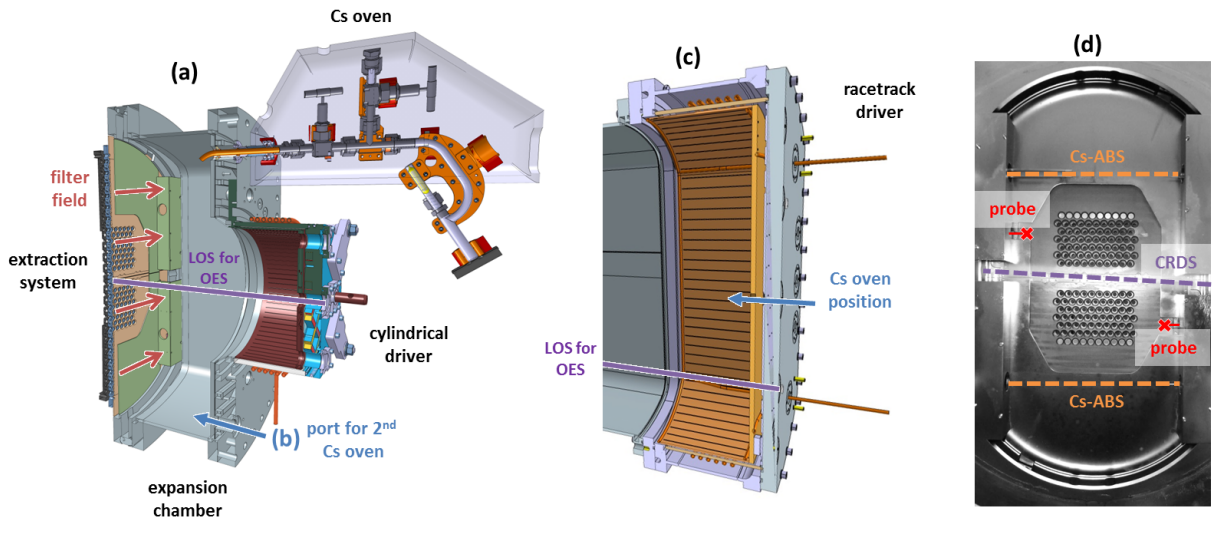

FIGURE 1. (a): sketch of the prototype source at BATMAN in standard configuration. (b) indicates the port used for installing a second Cs oven. (c) shows the racetrack driver, substituting the cylindrical driver. (d): view onto the PG with the measurement positions of the diagnostics indicated.

Since many years, the prototype source is attached to the BATMAN (Bavarian Test Machine for Negative ions) test facility [3]. Due to the flexible access for diagnostics as well as for the exchange of source components, BATMAN is ideally suited for investigation of the important physics of the ion source as well as for improving its design; the latter in particular also for possible NBI systems for fusion reactors beyond ITER. The influence of two modifications to the prototype source at BATMAN on plasma parameters is presented in this paper:

Firstly, a second Cs oven has been mounted in the bottom part of the expansion chamber in addition to the standard oven in the top part. Although it has been shown that Cs is distributed almost vertically symmetric during plasma phases close to the PG [8], this behavior differs after changing the magnetic filter field configuration from the more flexible external frame [9] to the standard configuration with internal magnets in the diagnostic flange. In the standard configuration the plasma drift is more pronounced and consequently the vertical Cs distribution in front of the PG is found to be more asymmetric in the drift direction. Since also the extracted negative ion beam is found to be significantly asymmetric (in the direction of the plasma drift) [10], a possible hypothesis was that the asymmetric Cs distribution might lead to an asymmetry of the work function of the PG and for this reason to an asymmetric production of H^-, limiting the total performance of the ion source. In order to check this hypothesis, a second Cs oven has been mounted in the bottom part of the expansion vessel. The possibility to control the Cs asymmetry in the source using both ovens and its effect on the source performance is presented.

Secondly, the cylindrical driver (Ø = 24.5 cm, volume of 7.5 l) has been exchanged by a much larger racetrack-shaped driver (area of 32 × 58 cm^2, volume of 38 l) [11]. The reason for testing a larger RF driver is a possible enhancement of the RF power efficiency in larger sources (the ITER source is based on a modular concept of eight cylindrical RF drivers) when substituting two cylindrical drivers with one racetrack driver. An increased RF power efficiency is highly desirable in order to increase the reliability of the ion source regarding RF issues at high power [12]. A high reliability is required for future NBI systems beyond ITER (based on the concept of the ITER sources). A comparison of the source performance for both cases can be found in [11]; this paper focuses on the comparison of plasma parameters in the driver as well as close to the plasma grid for both driver geometries.

EXPERIMENTAL SETUP

BATMAN is a pulsed-driven test facility with plasma pulses of ≈ 7 s length including 4.5 s beam extraction and a vacuum phase of typically 3-4 min between two pulses. A sketch of the ion source of BATMAN in the standard configuration is shown in Fig. 1 (a). One Cs oven is attached to the back plate of the expansion chamber in the top part of the source. Its nozzle is bent downwards, thus evaporating Cs directly onto the PG in the present configuration. The magnetic filter field is created by internal magnets mounted at an axial distance of 3 cm to the PG. An axial line of

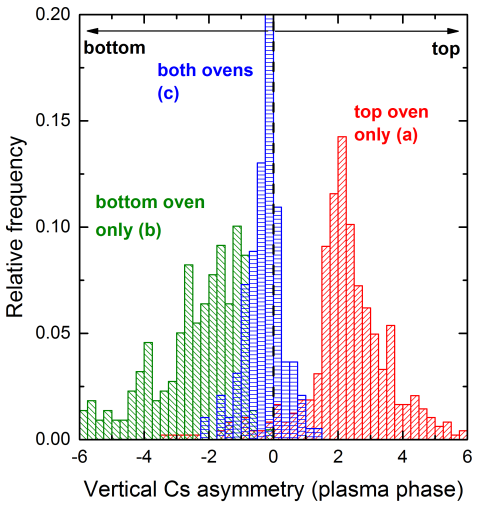

FIGURE 2. Histogram of the vertical neutral Cs asymmetry during plasma phases for three cases: Cs evaporation only from the top oven (a), only from the bottom oven (b) and using both ovens simultaneously (c).

sight (LOS) through the center of the driver is used for the characterization of the driver plasma by means of optical emission spectroscopy (OES). The first modification of the standard setup was the installation of a second Cs oven in port (b) indicated in Fig. 1. The second Cs oven uses a slightly different nozzle design: its nozzle consists of a straight tube which end is cut at a 45° angle facing to the upper part of the source. The second modification was the substitution of the cylindrical driver by the racetrack-driver shown in Fig. 1 (c). In this configuration, a 5 cm shorter expansion vessel has been used in order to keep the length between the PG and the back plate of the driver similar as in the standard configuration. For the racetrack driver, one Cs oven is mounted in the center of its back plate. The nozzle of the Cs oven is straight, thus Cs is evaporated symmetrically into the source. An axial LOS in the bottom part of the driver is used for the driver characterization by OES. A collisional radiative model is applied for determining plasma parameters from the measured emissivities (atomic H_α, H_β, H_γ and molecular Fulcher band) [13]. This allows to determine the electron temperature T_e, electron density n_e and the atomic to molecule ratio n_H/n_{H_2}.

The measurement positions of additional diagnostics close to the PG are shown in Fig. 1 (d). The neutral Cs density is measured by a tunable diode laser laser absorption diagnostics [14] at two vertically symmetric, horizontal LOS at an axial distance of 2.2 cm to the PG (Cs-ABS). The H^- density is measured at a vertically centered, horizontal LOS with the same axial distance of 2.2 cm to the PG by means of cavity ring-down spectroscopy (CRDS) [15]. The positive ion density is determined by two non-RF compensated Langmuir probes (symmetrically mounted) at a distance of 0.7 cm to the PG. The probes use a tungsten tip of 300 μm diameter and a length of 1 cm; a modified orbital motion limited (OML) fit [16] is applied to the positive ion branch of the recorded I-V-characteristic for the determination of the positive ion density n_i.

RESULTS

Variation of the Cs evaporation asymmetry

The vertical asymmetry of neutral Cs during plasma phases, defined as $S_{y,Cs} = (n_{Cs,top} - n_{Cs,bot})/\min(n_{Cs,top}, n_{Cs,bot})$, with $n_{Cs,top}$ and $n_{Cs,bot}$ the Cs density at the top and bottom LOS determined by Cs-ABS, can be clearly controlled using both ovens: a histogram of $S_{y,Cs}$ is plotted in Fig. 2. Several days of operation are compared, in which the cases of either using only the top oven (a), or only the bottom oven (b), or using both ovens simultaneously (c) are labeled. In case (a), the maximum of the relative frequency appears for a Cs asymmetry between 1.5 and 2.5; thus the neutral Cs density is usually a factor of 2.5–3.5 higher at the top LOS compared to the bottom LOS. In case (b), a broader maximum appears for values of $S_{y,Cs}$ clearly below zero (-3 – -0.75); thus the Cs asymmetry is shifted to the bottom in this case. The cases top oven only (a) and bottom oven only (b) are not perfectly mirrored because of two reasons: firstly, the two ovens are not using the same nozzle geometry. Secondly, the plasma drift to the top part of the source

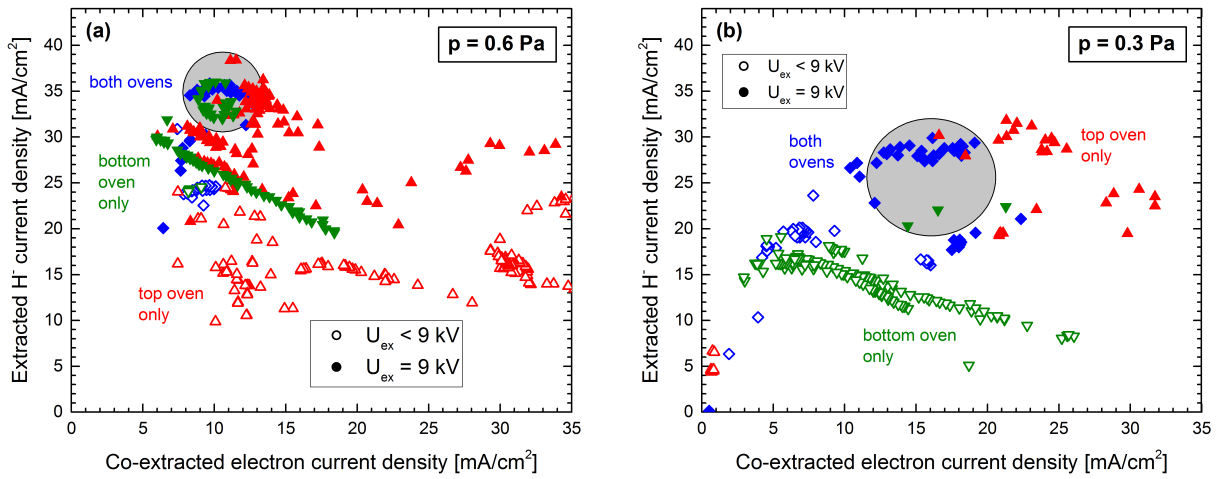

FIGURE 3. Performance plots of BATMAN, distinguishing the cases: Cs evaporation only from the top oven (red), only from the bottom oven (green) and using both ovens simultaneously (blue). Filled symbols denote an extraction voltage of 9 kV, open symbols a lower value of the extraction voltage. A filling pressure of 0.6 Pa has been used in (a); (b) shows the results for 0.3 Pa. The best pulses are highlighted in a grey ellipsis.

affects the redistribution processes of Cs seeded to the surfaces in the expansion chamber (the strong influence of the plasma phases on the redistribution of Cs can be found in [8]). In case (c) of using both ovens, a narrow maximum of the relative frequency appears for a Cs asymmetry close to zero. This was aimed in case (c), where the evaporation rates of the ovens has been adjusted in order to reach an almost symmetric distribution of neutral Cs during plasma phases. As regularly seen at BATMAN, the absolute density of neutral Cs has been in the order of 1×10^{15} m^{-3} (whereas in case (a) $n_{\mathrm{Cs,top}}$ is usually slightly higher and $n_{\mathrm{Cs,bot}}$ sligthly lower than this value; and vice versa for case (b)).

The influence of the variation of the Cs asymmetry on the source performance is shown in the performance plots of Fig. 3, in which the extracted H^- current density j_{H^-} is plotted as a function of the co-extracted electron current density j_e. In case of a filling pressure of 0.6 Pa (Fig. 3a), a similar source performance can be reached for all three oven configurations ($j_{H^-} \approx 35$ mA/cm^2, $j_e \approx 10$ mA/cm^2). Thus, the source performance is not limited by the asymmetry of Cs. In addition, also the beam profile and shift stays the same for these three configurations [17]. In case of 0.3 Pa filling pressure (Fig. 3b), a similar performance is reached using either the top oven only or using both ovens ($j_{H^-} \approx 30$ mA/cm^2, $j_e \approx 12 - 17$ mA/cm^2). Generally, the maximum reachable source performance is worse at the lower filling pressure. At 0.3 Pa, the best reached source performance using only the bottom oven is significantly lower compared to the other cases (extracted H^- current density of 22 mA/cm^2 instead of 29 mA/cm^2). Although spending more time for conditioning the source might have led to a better source performance in this case, it clearly seems that evaporating Cs onto surfaces in counter direction to the plasma drift is the worst of these cases. Since the redistribution of Cs by the plasma is the most important aspect of the Cs dynamics in the prototype source [8], Cs should be seeded on areas with sufficient plasma contact. In this case, the position of the oven is less relevant. Thus, in the standard configuration of the prototype source (plasma drift upwards, Cs oven mounted in the top) the determined Cs asymmetry does not significantly affect the source performance.

Comparison of two driver geometries

Figure 4a shows the source performance (j_{H^-} and j_e) as a function of the applied RF power for the cylinder driver and the racetrack driver at a filling pressure of 0.6 Pa. The pressure of 0.6 Pa has been chosen for this comparison since Cu sputtering from the inner surfaces of the expansion vessel lowered significantly the achievable source performance at 0.3 Pa in the racetrack driver. This issue does not play a role for the much smaller cylinder driver. To avoid Cu sputtering in the future, it is planned to cover the inner surfaces of the expansion vessel with molybdenum. The extracted negative ion current density is plotted in this figure for an extraction voltage of 5 kV as well as for 9 kV; for all following pulses it has been set to 5 kV in order to operate at the optimum of the perveance. For the cylinder

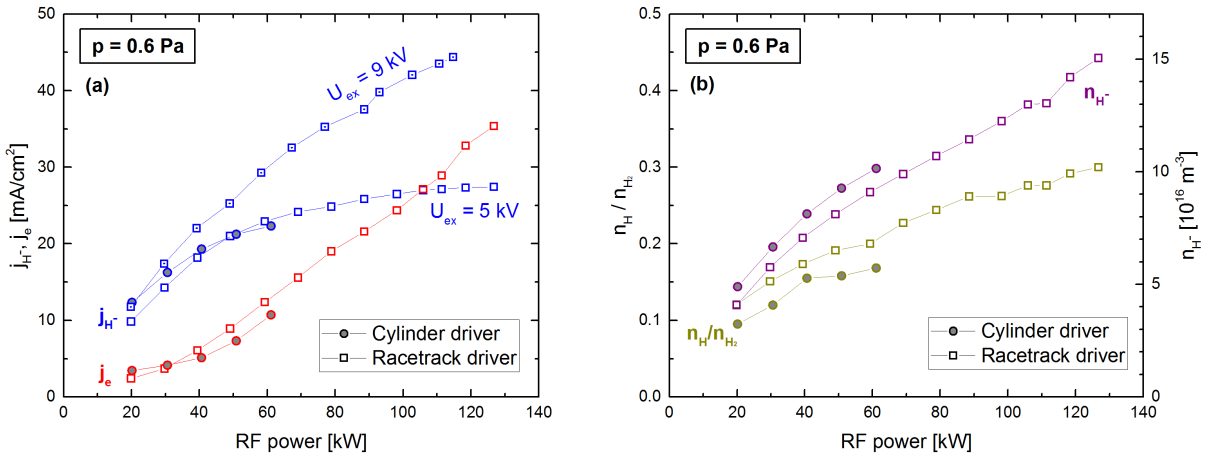

FIGURE 4. Comparison of the cylinder and the racetrack driver for varying RF power: (a) extracted H^- current density j_{H^-} for U_{ex} = 5 kV(racetrack and cylinder driver) and 9 kV (only racetrack driver), co-extracted electron current density j_e for U_{ex} = 5 kV. (b): atomic hydrogen fraction n_H/n_{H_2} in the driver and H^- density n_{H^-} in front of the PG.

driver, the maximum applied RF power was limited to ≈ 60 kW due to the available RF generator in this campaign; in principle it is possible to apply a RF power of up to ≈ 100 kW to the cylinder driver. For the racetrack driver, a 150 kW RF generator was used and a power of up to 130 kW was applied. The source performance is similar for both drivers (U_{ex} = 5 kV). The extracted negative ion current density starts saturating at a power level of ≈ 80 kW for U_{ex} = 5 kV, whereas j_{H^-} shows no saturation at an extraction voltage of 9 kV.

In addition to the H^- density n_{H^-} in front of the plasma grid, Fig. 4b shows the ratio of hydrogen atoms to molecules n_H/n_{H_2} in the driver for the same comparison as in Fig. 4a (U_{ex} = 5 kV). The negative hydrogen ion density is similar for both drivers and shows exactly the same trend as j_{H^-} at U_{ex} = 9 kV. Thus, the saturation of j_{H^-} at U_{ex} = 5 kV for high RF power must be based on either space charge limiting effects or attributed to a different shape of the plasma meniscus (which is the transition between the quasi-neutral plasma and the extracted particle beam in front of each extraction aperture). The ratio n_H/n_{H_2} is similar or slightly higher for the racetrack driver and shows the same trend as the H^- density in front of the PG. Since both quantities do not saturate even at large values of the applied RF power, neutral depletion [18] seems to play a minor role in the larger racetrack driver.

A comparison of both drivers regarding the electron density n_e in the driver and the positive ion density n_i in front of the PG (top and bottom Langmuir probe position) is shown in Fig. 5. All densities increase with higher applied RF power. Whereas n_e is higher in the cylinder driver than in the racetrack driver, the positive ion densities in front of the PG are very similar for both cases. Remarkably, the vertical plasma asymmetry in front of the PG is very similar for both drivers. This is a clear indication that the plasma asymmetry in front of the PG is solely determined by the magnetic filter field.

A comparison of the plasma parameters for both drivers in the case of 60 kW RF power is shown in Table 1, in which additionally the determined electron temperature T_e in the driver is given. The electron density is 65% higher in the cylinder driver, what is explained by the five times higher RF power density in the smaller cylinder driver. In contrary, the ratio n_H/n_{H_2} is similar or even slightly higher in the racetrack driver, which is attributed to an increased volume/surface ratio and thus less losses of hydrogen atoms at the wall due to recombination. The electron temperature is the same for both drivers at 0.6 Pa (10 eV). The plasma density from the driver to the PG is reduced less with the racetrack driver, which might be caused by the shorter expansion vessel and thus a shorter diffusion length. A future comparison for the same expansion length is foreseen.

Figure 6 shows a comparison of the plasma parameters n_H/n_{H_2} and n_e for both drivers and two filling pressures (0.3 Pa and 0.6 Pa) as function of the applied RF power. This comparison is only done for plasma parameters in the driver, because – as mentioned before – Cu sputtering limited the source performance at 0.3 Pa with the racetrack driver. In particular at higher values of the RF power, a slightly higher ratio n_H/n_{H_2} is observed at lower pressure; this tendency applies for both drivers. As already discussed for 0.6 Pa, also for 0.3 Pa no saturation of n_H/n_{H_2} takes place in the applied power range. As expected, the electron density is decreased for the lower filling pressure in both drivers.

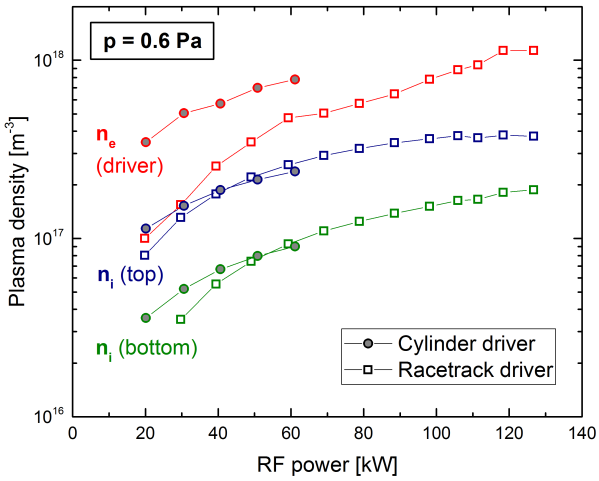

FIGURE 5. Comparison of the cylinder and the racetrack driver for varying RF power: electron density in the driver n_e as well as the positive ion density n_i in front of the plasma grid (top and bottom position).

The relative decrease, however, is stronger pronounced for the cylinder driver: at 50 kW RF power, n_e is decreased by 50% in the cylinder driver (0.6 Pa → 0.3 Pa), whereas it is only decreased by 22% in the racetrack driver. The electron temperature is – independent of the applied RF power – slightly higher in the cylindrical driver (12 eV) compared to the racetrack driver (10 eV) at 0.3 Pa.

The main aspect of the driver in caesiated negative ion sources is the dissociation of hydrogen molecules into atomic species. Thus, achieving a similar or even higher value of n_H/n_{H_2} at the same RF power with the racetrack driver compared to the cylinder driver is a promising result for the application of the racetrack driver in larger sources for negative hydrogen ions.

SUMMARY

Two modifications of the standard prototype source have been tested at the BATMAN test facility:

The installation of a second Cs oven in the bottom part of the source (in addition to the standard oven in the top part) led to the possibility to control the vertical asymmetry of neutral Cs in plasma phases. However, varying the vertical Cs asymmetry does not significantly change the maximum reachable source performance – with one exception: evaporation from only the bottom oven in counter direction to the plasma drift to the top part seems leading to a significantly worse source performance at a filling pressure of 0.3 Pa. Nevertheless, the standard configuration with only one oven in the top part of the source is sufficient to achieve the maximum source performance. The position of the Cs oven is less relevant as long as Cs is deposited on areas with sufficient plasma contact for redistribution.

Exchanging the cylindrical driver with a much larger racetrack-shaped driver led to promising results for the possibility of substituting two cylindrical drivers with one racetrack driver in larger ion sources: whereas the electron density at the same applied RF power is significantly lower in the racetrack driver, attributed to the much lower RF power density, the ratio of hydrogen atoms to molecules is similar or even slightly increased. This leads to a similar source performance of both drivers at a filling pressure of 0.6 Pa; for lower filling pressure operation in the racetrack driver has been hampered by Cu sputtering from the expansion vessel. For mitigation of the latter, a Mo coating will

TABLE 1. Comparison of plasma parameters n_e, n_H/n_{H_2} and T_e in the driver, n_i in front of the plasma grid, as well as the power density (RF power per volume) for the cylinder and the racetrack driver. 60 kW RF power, 0.6 Pa filling pressure.

	n_e	n_H/n_{H_2}	T_e	n_i (top)	n_i (bottom)	RF power density
Cylinder driver	7.8×10^{17} m^{-3}	0.17	10 eV	2.4×10^{17} m^{-3}	0.90×10^{17} m^{-3}	8.0 kW/l
Racetrack driver	4.7×10^{17} m^{-3}	0.20	10 eV	2.6×10^{17} m^{-3}	0.93×10^{17} m^{-3}	1.6 kW/l

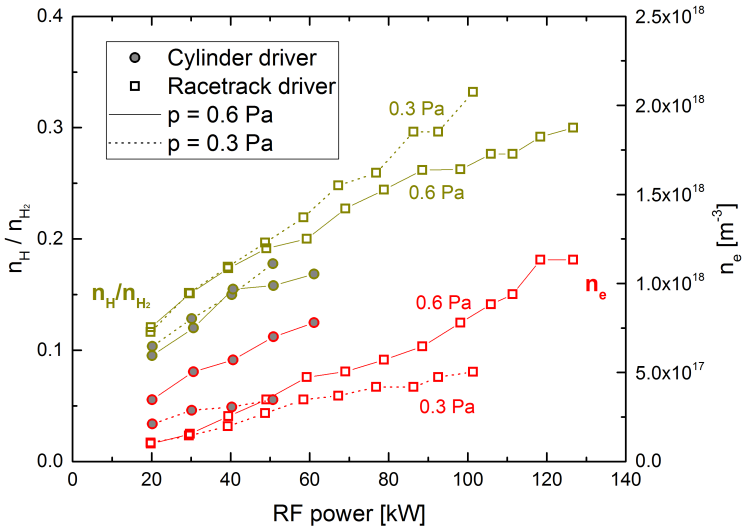

FIGURE 6. Plasma parameters in the driver (n_e and n_H/n_{H_2}) comparing two pressures (0.3 Pa and 0.6 Pa) for the cylinder and the racetrack driver.

be applied to the inner walls of the expansion chamber. Remarkably the plasma asymmetry in front of the plasma grid is similar for both drivers – leading to the assumption that the plasma asymmetry close to the PG is solely determined by the magnetic filter field.

ACKNOWLEDGMENTS

This work has been carried out within the framework of the EUROfusion Consortium and has received funding from the Euratom research and training programme 2014-2018 under grant agreement No 633053. The views and opinions expressed herein do not necessarily reflect those of the European Commission.

REFERENCES

[1] R. Hemsworth, H. Decamps, J. Graceffa, B. Schunke, M. Tanaka, M. Dremel, A. Tanga, H. D. Esch, F. Geli, J. Milnes, T. Inoue, D. Marcuzzi, P. Sonato, and P. Zaccaria, Nucl. Fusion **49**, p. 045006 (2009).
[2] B. Schunke, D. Bora, R. Hemsworth, and A. Tanga, AIP Conf. Proc. **1097**, 480–490 (2009).
[3] E. Speth, H. Falter, P. Franzen, U. Fantz, M. Bandyopadhyay, S. Christ, A. Encheva, M. Fröschle, D. Holtum, B. Heinemann, W. Kraus, A. Lorenz, C. Martens, P. McNeely, S. Obermayer, R. Riedl, R. Süss, A. Tanga, R. Wilhelm, and D. Wünderlich, Nucl. Fusion. **46**, p. S220 (2006).
[4] R. S. Hemsworth, A. Tanga, and V. Antoni, Rev. Sci. Instrum. **79**, p. 02C109 (2008).
[5] M. Bacal and M. Wada, Appl. Phys. Rev. **2**, p. 021305 (2015).
[6] D. Wünderlich, R. Gutser, and U. Fantz, Plasma Sources Sci. Technol. **18**, p. 045031 (2009).
[7] U. Fantz, L. Schiesko, and D. Wünderlich, Plasma Sources Sci. Technol. **23**, p. 044002 (2014).
[8] C. Wimmer, U. Fantz, and NNBI-Team, AIP Conf. Proc. **1515**, 246–254 (2013).
[9] P. Franzen, L. Schiesko, M. Fröschle, D. Wünderlich, U. Fantz, and NNBI Team, Plasma Phys. Controlled Fusion **53**, p. 115006 (2011).
[10] R. Maurizio, U. Fantz, F. Bonomo, and G. Serianni, Nucl. Fusion **56**, p. 066012 (2016).
[11] W. Kraus *et al.*, contribution to the NIBS 2016 conference, AIP Conf. Proc. **this volume** (2017).
[12] D. Wünderlich, W. Kraus, M. Fröschle, R. Riedl, U. Fantz, B. Heinemann, and NNBI Team, contribution to the NIBS 2016 conference, AIP Conf. Proc. **this volume** (2017).
[13] D. Wünderlich, S. Dietrich, and U. Fantz, Journal of Quantitative Spectroscopy & Radiative Transfer **110**, 62–71 (2009).
[14] U. Fantz and C. Wimmer, J. Phys. D: Appl. Phys. **44**, p. 335202 (2011).

[15] M. Berger, U. Fantz, S. Christ-Koch, and NNBI Team, Plasma Sources Sci. Technol. **18**, p. 025004 (2009).
[16] F. Chen, Plasma Sources Sci. Technol. **18**, p. 035012 (2009).
[17] E. Aza, D. Wünderlich, L. Schiesko, and C. Wimmer, contribution to the NIBS 2016 conference, AIP Conf. Proc. **this volume** (2017).
[18] P. McNeely, D. Wünderlich, and NNBI Team, Plasma Sources Sci. Technol. **20**, p. 045005 (2011).